ELSEVIER

Available online at www.sciencedirect.com
SCIENCE DIRECT

Journal of Crystal Growth 276 (2005) 525–533

JOURNAL OF CRYSTAL GROWTH

www.elsevier.com/locate/jcrysgro

Microstructural evolution and formation of highly *c*-axis-oriented aluminum nitride films by reactively magnetron sputtering deposition

Wen-Jen Liu[a,*], Shih-Jeh Wu[b], Chih-Min Chen[c], Yin-Chieh Lai[c], Chun-Han Chuang[a]

[a]*Department of Material Science and Engineering, I-Shou University, No. 1, Section 1, Hsueh-Cheng Road, Ta-Hsu Hsiang, Kaohsiung, 84008 Taiwan, ROC*
[b]*Department of Mechanical and Automation Engineering, I-Shou University, Kaohsiung, Taiwan, ROC*
[c]*Institute of Electro-Optical Engineering, National Chiao Tung University, Hsinchu, Taiwan, ROC*

Received 8 October 2004; accepted 29 November 2004
Communicated by R. Kern
Available online 1 January 2005

Abstract

Highly (0 0 2) *c*-axis-oriented AlN films have been successfully deposited on Ti/Si substrates using reactive magnetron radio frequency (RF) sputtering deposition and ideal AlN films could be obtained by fine-tuning the parameters at pressure 5 Pa, temperature of 250 °C, and N_2 ratio 85%. The detailed layer-by-layer microstructure of AlN films deposited on Ti/Si substrate consists of TiO_2 thin film, amorphous layer without Al_2O_3 particles, transition layer, and the columnar (0 0 2) *c*-axis preferred orientation layer.

AlN films possessing a higher deposition rate to form an amorphous layer in the initial deposition stage will result in the lower deposition rate to form following transition and columnar preferred orientation textures. Therefore, we strongly suggest adopting a two-step deposition method, that is, use lower deposition rate to form preferred orientation layers and then a higher deposition rate to form preferred orientation textures.
© 2004 Elsevier B.V. All rights reserved.

PACS: 81.15.Cd; 68.35.Bs; 68.35.Ct; 68.55.Jk

Keywords: A1. Growth mechanism; A1. Transmission electron microscopy; A3. Reactive sputtering; B2. Aluminum nitride

*Corresponding author. Tel.: +886 7 6577262; fax: +886 7 6578444.
E-mail address: jurgen@isu.edu.tw (W.-J. Liu).

0022-0248/$ - see front matter © 2004 Elsevier B.V. All rights reserved.
doi:10.1016/j.jcrysgro.2004.11.421

1. Introduction

Highly *c*-axis (0 0 2) oriented aluminum nitride (AlN) film is a candidate material of surface acoustic wave (SAW) and film bulk acoustic resonator (FBAR) devices for its excellent piezoelectricity, stable chemical property and high acoustic wave velocity [1,2]. For higher carrier frequencies (>5 GHz) of mobile telecommunication applications, AlN films are expected to replace the submicron process development in SAW devices.

Recent interest mainly focuses on preciously controlling piezoelectric properties by process parameters such as distance between substrate and target, wattage, N_2 gas ratio, substrate temperature, substrate roughness, bias and operating pressure. In order to be properly selective for wireless communication devices, polycrystalline AlN films must satisfy two basic requirements: the (0 0 2) *c*-axis textures have to be perpendicular to the substrate, which is referred to as *c*-axis preferred orientation, and the AlN films must have void-free columnar structures and reasonable composition. It is recognized that roughness, structure, and thickness of electrode metal also result in difference in formation of highly *c*-axis AlN films [3]. AlN possesses hexagonal structures that preferentially grow to the *c*-axis preferred orientation on various metals such as platinum (Pt), aluminum (Al) and gold (Au) for their lattice match. Meanwhile, Pt and Au films are difficult to be directly deposited on substrates and to be etched, and Al has problems of the surface oxidation and the etching selectivity with AlN film. Titanium (Ti) exhibits a hexagonal structure similar to that of AlN and better etching selectivity. Therefore, in this study we adopt e-beam deposition to evaporate lower roughness Ti as bottom electrode metal.

Generally, AlN films can be synthesized using several techniques, such as reactive sputtering [4–7], molecular beam epitaxy [8], laser ablation [9], chemical vapor deposition (CVD) [10,11], and plasma-enhanced CVD [12]. Among these methods, the reactive magnetron sputtering technique is considered to be the favorable selection due to its easily deposited high *c*-axis orientation and its high growth rate. In this study, a self-designed reactive magnetron sputtering system, as shown in Fig. 1, was used to deposit AlN films. The film grown by the system has lower growth rate, higher density, and smoother surface. Furthermore, it was found that (0 0 2) *c*-axis preferred orientation existed even near room temperature. Simultaneously, Hwang et al. [6] have reported that the detailed layer-by-layer microstructure of AlN films

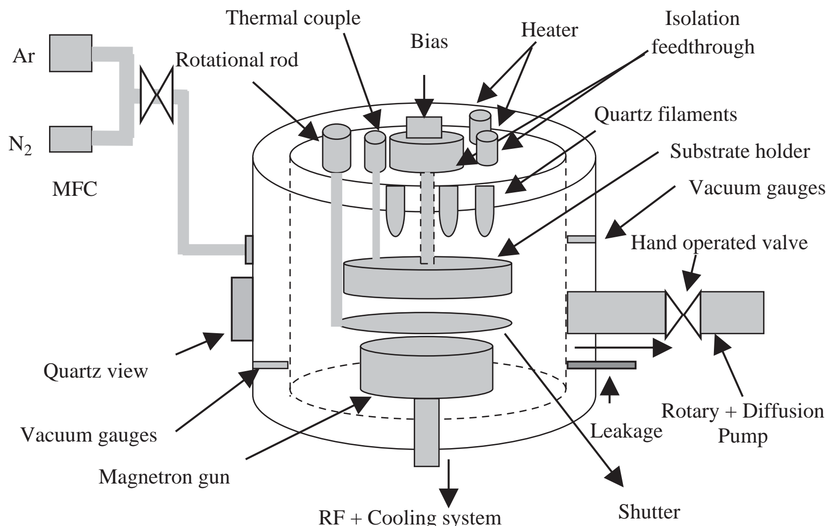

Fig. 1. Schematic diagram of the reactively magnetron RF sputtering deposition system.

deposited on amorphous SiO_2/Si substrate consists of amorphous layer with alumina (Al_2O_3) particles, transition layer, and columnar layer. While the real FBAR device with bottom electrode metal condition may reveal other information, we also use cross-sectional transmission electron microscopy (XTEM) for microstructural evolution of the radio frequency (RF) reactively deposited AlN films on Ti/Si substrate with the designed thickness by MATLAB6.5 software calculation. From the selected area diffraction (SAD) analysis of TEM, the growth mechanism is also proposed by the microstructural observations.

2. Experimental procedures

2.1. Substrates preparation and deposition

P-type (1 0 0) silicon samples of area 40 mm × 40 mm and thickness 0.55 mm, were cleaned by the ultrasonic baths of acetone, isopropylalcohol, methanol, and de-ionized water. Subsequently, they were blown out with dry nitrogen gas and heated on a hot plate at a temperature of 50 °C for 1 min before performing titanium metal deposition. Finally, the same low roughness substrates are obtained by depositing 80 nm thickness titanium metal via electron beam evaporation (EBE) at a fixed deposition rate of 0.3 nm/s.

The AlN films were deposited on Ti/Si substrates in a reactive magnetron RF sputtering chamber in a gas mixture of high purity (99.999%) argon and nitrogen. The aluminum target was 50 mm in diameter, 6 mm in thickness and a purity of 99.999%. After the vacuum chamber was evacuated below 8.0×10^{-4} Pa, the substrates were sputter cleaned for 15 min using argon plasma prior to film deposition for removing oxide and contamination. The substrates were heated by quartz filaments to control the temperatures at 50, 150, 250, and 350 °C. The target to substrate distance and the RF wattage were kept constant at 50 mm and 165 W, respectively. The deposition time was set at 6 h for each sample.

2.2. Design of experiment and material analysis

Initially, the experiment followed the orthogonal array method [13] and other studies [14,15] by

Table 1
Orthogonal array design of experiments and effect of process parameters on the roughness and compositions of AlN films

Sample no.	Pressure (Pa)	Temperature (°C)	N_2 gas ratio (%)	Roughness (nm)	N/Al ratio
(I)	2	400	75	—	—
(II)	1	350	75	—	—
(III)	2	350	70	—	—
(IV)	1	400	70	—	—
(1)	0.13	350	75	2.852	0.431271
(2)	0.26	350	75	3.271	0.543386
(3)	0.50	350	75	3.483	0.661958
(4)	0.60	350	75	3.612	0.650712
(5)	0.73	350	75	3.826	0.610352
(6)	1.00	350	75	4.172	0.557147
(7)	1.27	350	75	4.571	0.521167
(8)	2.00	350	75	4.974	0.486619
(9)	2.67	350	75	5.221	0.407658
(10)	0.50	50	75	2.164	0.484781
(11)	0.50	150	75	2.616	0.604107
(12)	0.50	250	75	3.159	0.691189
(13)	0.50	250	85	4.376	0.728310
(14)	0.50	250	50	3.040	0.691189
(15)	0.50	250	25	2.781	0.642576

The target to substrate distance, RF wattage, and deposition time were maintained constant at 50 mm, 165 W, and 6 h, respectively.

varying parameters such as operating pressure, substrate temperature, and N_2 gas ratio to find out the best combination on the preferred orientation of AlN film, parameters symbols (I–IV) as shown in Table 1. Subsequently, these parameters were varied step by step for identifying the optimum process parameters. Finally, the film structure and preferred orientation were measured by an X-ray diffractometer (Scintag Inc., USA) operated at 35 kV and 30 mA. Surface roughness of the films was measured under $2\,\mu m \times 2\,\mu m$ size using an atomic force microscope (AFM, Solver Scanning probe microscope SPM-P7LS). Film topography and compositional analysis were performed by a scanning electron microscope (SEM, JSM-6400) and X-ray photoelectron spectroscopy (XPS, VG.ESCA210 electron spectroscopy for chemical analysis), respectively. XTEM samples were prepared by cutting, mechanical grinding, chemical mechanical polishing, and ion-milling (Gatan Duo-mill) to electron transparency. High-resolution transmission electron microscopy (HRTEM) with energy dispersive spectroscopy (EDS) was used to observe the cross-sectional microstructure of AlN thin films with a JEOL JEM-4000EX type electron microscope operated at a voltage of 400 kV. The results were compared with the reports of AlN films deposited by other reactive sputtering techniques, and the kinetic formation of highly *c*-axis (0 0 2) oriented AlN films was discussed.

3. Results and discussions

3.1. XRD analysis of orthogonal array method design

Based on the results of Kao et al. [14] and Cheng et al. [15], it was indicated that operating pressure, substrate temperature, and N_2 gas ratio are the main factors affecting the preferred orientation AlN films. Therefore, we followed the orthogonal array method, as shown in Table 1, and found highly (0 0 2) *c*-axis-oriented AlN films with minor other crystallite planes occurring at pressure 0.5 Pa, temperature of 350 °C, and N_2 ratio 75%, as shown in Fig. 2 (a). Subsequently, we varied these parameters step by step for identifying the optimum process parameters of highly (0 0 2) *c*-axis-oriented AlN films.

3.2. Effect of detail parameters variations on AlN films

3.2.1. XRD analysis

Fig. 2(b) shows the dependence of the (0 0 2) *c*-axis preferred orientation on operating pressure at fixed temperature 250 °C and N_2 gas ratio 75%. It was evident that 0.5 Pa pressure gave better performance. The results can be explained by considering the change of atom scattering and plasma glow discharge with the operating pressure. Atom scattering between sputtered atom and gas molecules increase with increasing gas pressure and result in the insufficient energy in deposited atoms, which has a negative effect on the preferred orientation. Meanwhile, unstable plasma glow discharge occurred at low operating pressures of 0.13 and 0.26 Pa, and also resulted in less preferred orientation.

Subsequently, we changed the substrate temperature from 50 to 350 °C, and maintained the operating pressure and the nitrogen partial pressure constant at 0.5 Pa and 75%, respectively. It appeared that there was higher preferred orientation at 250 °C as shown in Fig. 2(c). The phenomenon can be explained by considering variations of atom mobility and escape. Increasing substrate temperature increases the arriving atom mobility and results in a higher preferred orientation. Nevertheless, overmobile atoms increase the probability of the atoms escaping from the substrate surface, and this the results in lower preferred orientation.

Finally, we varied the N_2 gas ratio from 25% to 85%, and maintained the operating pressure and the substrate temperature constant at 0.5 Pa and 250 °C, respectively. This indicated that the 85% N_2 gas ratio has the higher preferred orientation, as shown in Fig. 2(c). The phenomenon can be explained by considering the sufficient nitrogen atoms. We also tried the 90% N_2 gas ratio and found the evident target poisoning phenomena resulting in AlN films cracking issues.

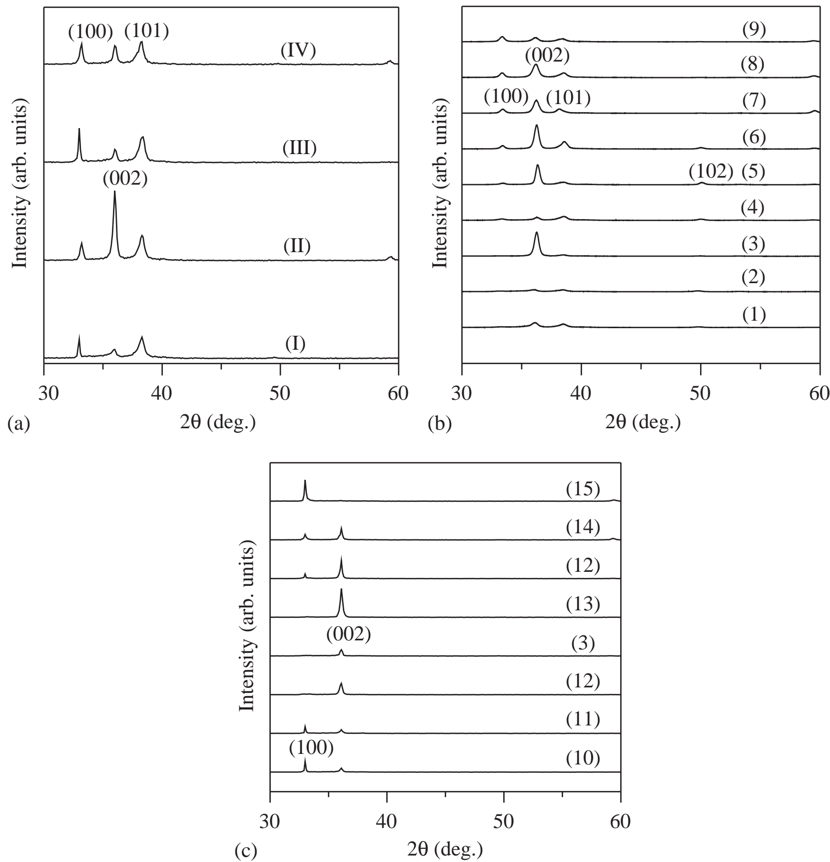

Fig. 2. XRD analysis of orthogonal array design of experiments, and the influences of operating pressure, substrate temperature, and N_2 gas ratio on preferred (0 0 2) *c*-axis orientation of AlN films. The detailed process parameter symbols are shown in Table 1.

Therefore, it is obviously indicated that the ideal AlN films could be obtained by fine-tuning the parameters at pressure 0.5 Pa, temperature of 250 °C, and N_2 ratio 85%.

3.2.2. *AFM, XPS, and SEM analysis*

Table 1 also indicates the influences of operating pressure, substrate temperature, and N_2 gas ratio on roughness and composition of AlN films. Collisions between electrons and gas molecules will increase with increasing gas pressure and result in a higher ion density and deposition rate; hence roughness will also increase. Increasing substrate temperature and N_2 gas ratio also has the same trends. AlN film compositions that were analyzed by XPS indicated that the ratio value of nitrogen to aluminum was insufficient.

Figs. 3 (a)–(d) revealed the SEM topography analysis of AlN films at pressure 0.5 Pa, temperature 250 °C, and N_2 gas ratios 50% and 85%, respectively. It was shown that columnar rounded crystals with many small grains formed grain boundary striations in top-view samples, and columnar growth crystals feature in cross-sectional samples. How the major randomly oriented micrograins in the transition layer connected and transferred to small grains with the same growth direction for reducing surface energy can be explained. Simultaneously, from the observation of AlN crystallization with FESEM, it was inferred that the longer deposition time resulted

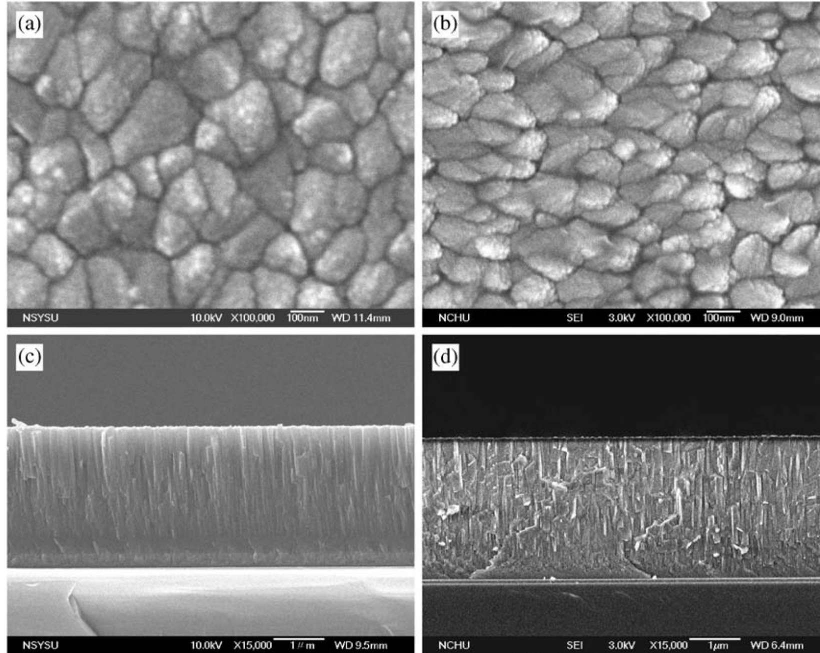

Fig. 3. SEM topography analysis of AlN films at fixed pressure 0.5 Pa, temperature 250 °C, and N_2 ratios 50% by (a) top view and (c) cross-sectional view; 85% (b) top view and (d) cross-sectional view.

in the crystallization growth and a better crystalline structure formed at an extended deposition time, and the crystalline growth rate increased with the deposition time, as shown in Fig. 4.

It is also obvious that the ideal AlN films can be obtained at pressure 0.5 Pa, temperature 250 °C, and N_2 gas ratio 85%.

3.3. *Microstructural evolution and growth mechanisms of AlN films*

HRTEM/EDS observations indicate that titanium oxide (TiO_2) was formed on titanium electrode metal, and thicknesses of TiO_2 and amorphous AlN layers were about 5.5 nm and 170 nm, respectively, as shown in Fig. 5. A thickness of about 500 nm AlN transition layer was found to form on the amorphous layer, and it showed that randomly oriented micro-grains were incorporated to construct the columnar grains. Columnar grains continuously merged and grew with increase in the thickness of AlN films.

Fig. 6 presents the analysis of SAD pattern, and indicates that the major randomly oriented micro-

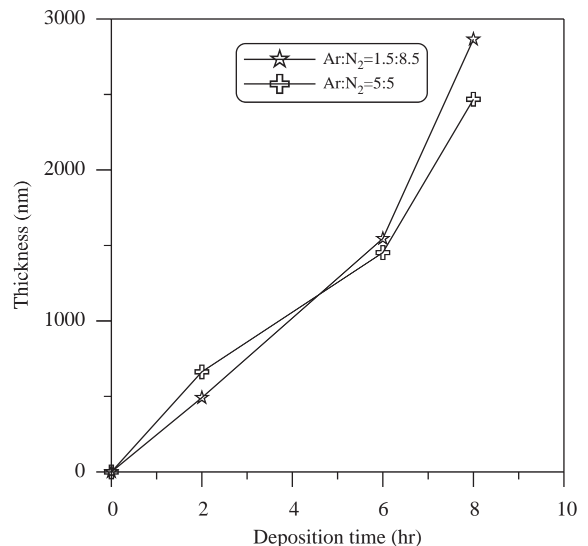

Fig. 4. Relationship between deposited thickness and deposition time.

grains with the maximum misaligned angle of 42° for the (0 0 2) textured direction was incorporated to construct the columnar grains. In the following

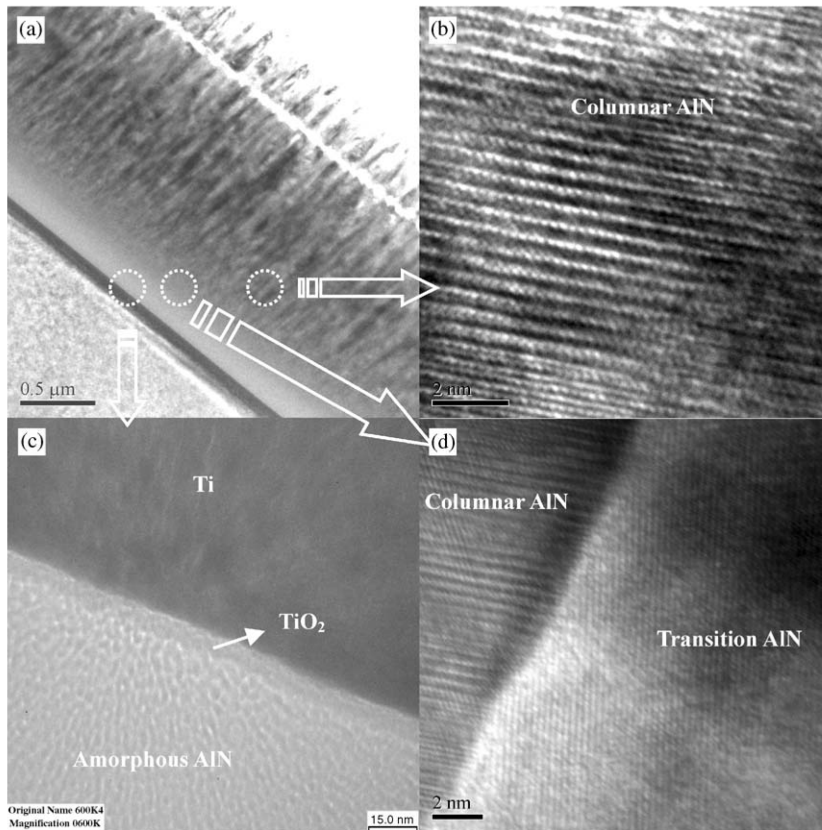

Fig. 5. HRTEM/EDS observations indicated that the cross-sectional feature of AlN films deposited on Ti/Si substrate consists of thin titanium oxide, amorphous layer without Al_2O_3 particles, transition layer, and columnar layer. (b), (c), and (d) Localized enlargements of (a).

growth, these micro-grains connected and transferred to small grains with the same growth direction for reducing surface energy. The misaligned angle had gradually decreased to 12°. Eventually, the single crystallization columnar grains formed with 4° misaligned angle.

Based on the above results, we proposed a growth mechanism of AlN films deposited on Ti/Si substrate, as indicated in Figs. 7(a) and (b). AlN films possessing a higher deposition rate to form an amorphous layer in the initial deposition stage will result in a lower deposition rate to form preferred orientation textures in the following deposition rate for later forming transition and columnar layers, as shown in Fig. 7(b). Therefore, we strongly suggest adopting a two-step deposition method, that is, a lower deposition rate to form preferred orientation layers and then a higher deposition rate to form preferred orientation textures. This will be considered by our next experiments.

The detailed layer-by-layer microstructure of AlN films deposited on Ti/Si substrate consists of TiO_2 thin film, amorphous layer without Al_2O_3 particles, transition layer, and columnar layer. The amorphous layer indicated different results from the study of Hwang et al. [6]; it is predicted the Ti and TiO_2 provide a great barrier for oxygen diffusion and prevent the formation of Al_2O_3 particles and lower residual O_2 gas in the chamber.

4. Conclusions

Highly (0 0 2) *c*-axis-oriented AlN films have been successfully deposited on the Ti/Si substrates using reactive magnetron RF sputtering

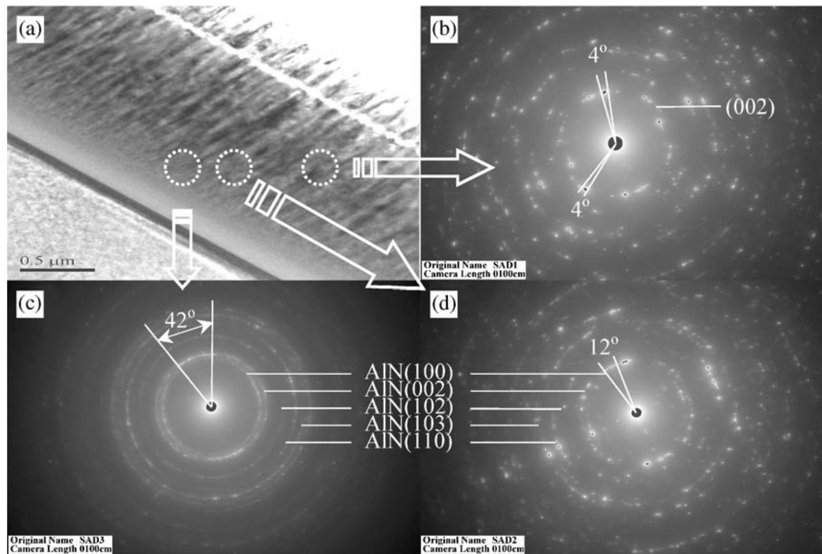

Fig. 6. Cross-sectional TEM analysis of AlN films. (b), (c), and (d) Localized SAD analysis of (a).

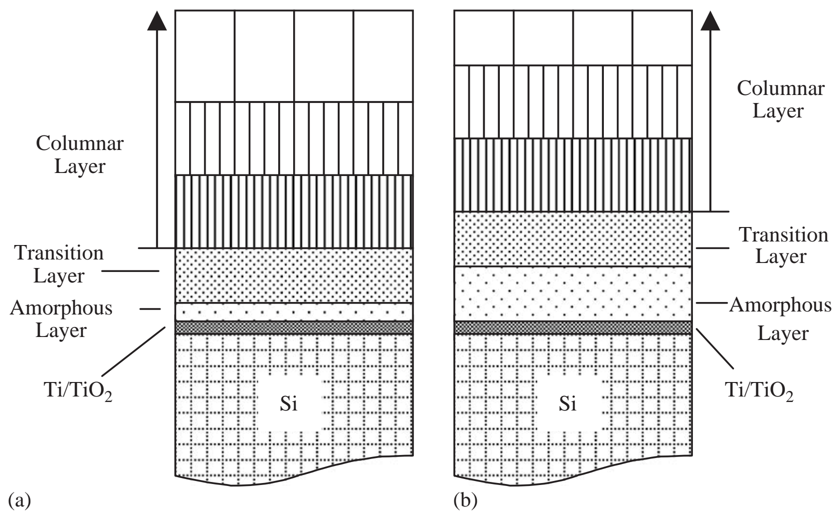

Fig. 7. Growth mechanism of AlN films deposited on Ti/Si substrate. (a) Low amorphous growth rate results in earlier formation of transition layer and preferred orientation columnar layer; (b) high amorphous growth rate results in later formation of transition layer and preferred orientation columnar layer.

deposition, and will be adopted to fabricate FBAR devices in our next research. The results of this study can be summarized as follows:

(1) From the orthogonal array experimental results, it appears that the highly (0 0 2) *c*-axis-oriented AlN films with minor other crystallite planes occurred at pressure 0.5 Pa, temperature of 350 °C, and N_2 gas ratio 75%. The ideal AlN films could be obtained by fine-tuning the parameters at pressure 0.5 Pa, temperature 250 °C, and N_2 ratio 85%.

(2) AlN films possessing a higher deposition rate to form an amorphous layer in the initial deposition stage will result in a lower deposition rate to form preferred orientation textures in the following deposition rate for later forming transition and columnar layers. Therefore, we strongly suggest adopting a two-step deposition method, that is, a lower deposition rate to form preferred orientation layers and then a higher deposition rate to form preferred orientation textures.
(3) The detailed layer-by-layer microstructure of AlN films deposited on Ti/Si substrate consists of TiO_2 thin film, amorphous layer without Al_2O_3 particles, transition layer, and columnar (0 0 2) *c*-axis preferred orientation layer.

Acknowledgement

The authors would like to thank Prof. Ro Ru-Yen of Communication Engineering Department of I-Shou University for fruitful directions and discussions. We gratefully acknowledge the support and discussions of manufacturing process in the National Nano Device Laboratory staff. This work was financially supported by the National Science Council of the Republic of China under Contract nos. NSC91-2213-E-214-024 and NSC92-2622-E-214-003-CC3.

References

[1] K. Tsubouchi, N. Mikoshiba:: IEEE Trans. Sonics Ultrason. SU 32 (1985) 634.
[2] R.B. Stokes, J.D. Crawford, IEEE Trans. Microwave Theory Technol. 41 (1993) 1075.
[3] S.H. Lee, J.K. Lee, Ki Hyun Yoon, J. Vac. Sci. Technol. A 21 (2003) 1.
[4] M. Ishihara, S.J. Li, H. Yumo, K. Akashi, Y. Ide, Thin Solid Films 316 (1998) 152.
[5] H.E. Cheng, T.C. Lin, W.C. Chen, Thin Solid Films 425 (2003) 85.
[6] B.H. Hwang, C.S. Chen, H.Y. Lu, T.C. Hsu, Mater. Sci. Eng. A 325 (2002) 380.
[7] S. Wu, L. Wu, F.C. Chang, J.H. Chang, Jpn. J. Appl. Phys. 40 (2001) 471.
[8] K.S. Stevens, A. Ohtani, M. Kinniburgh, R. Beresford, Appl. Phys. Lett. 65 (1994) 321.
[9] M. Okamoto, M. Yamaoka, Y.K. Yap, M. Yoshimura, Y. Mori, T. Sasaki, Diamond Rel. Mater. 9 (2000) 516.
[10] B. Aspar, R. Rodriguez-Clemente, A. Figueras, B. Armas, C. Combescure, J. Crystal Growth 129 (1993) 56.
[11] K. Kaya, H. Takahashi, Y. Shibata, Y. Kanno, T. Hirai, Jpn. J. Appl. Phys. 36 (1997) 307.
[12] J.W. Soh, S.S. Jang, I.S. Jeong, W.J. Lee, Thin Solid Films 279 (1996) 17.
[13] P.J. Ross, Taguchi Techniques for Quality Engineering, Second ed, McGraw-Hill, New York, 1996.
[14] K.S. Kao, C.C. Cheng, Y.C. Chen, IEEE Trans Ultrason. Ferroelectr. Freq. Control 49 (2002) 345.
[15] C.C. Cheng, Y.C. Chen, H.J. Wang, W.R. Chen, Jpn. J. Appl. Phys. 35 (1996) 1880.